

Manuscript Number:

Title: Data driven approach reveals oceanographic features delineate growth zonation in northeast pacific sablefish

Article Type: Research Paper

Keywords: growth; von Bertalanffy; ecosystem-based fisheries management; sablefish; spatiotemporal

Corresponding Author: Ms. Maia Sosa Kapur,

Corresponding Author's Institution:

First Author: Maia Sosa Kapur

Order of Authors: Maia Sosa Kapur; Melissa Haltuch; Brendan Connors; Luke Rogers; Aaron Berger; Jason Cope; Elliot Koontz; Katy Echave; Kari Fenske; Dana Hanselman; André E Punt

Manuscript Region of Origin: USA

Abstract: Renewed interest in the estimation of spatial and temporal variation in fish traits, such as body size, is a result of computing advances and the development of spatially-explicit management frameworks. However, many attempts to quantify spatial structure or the distribution of traits utilize a priori approaches, which involve pre-designated geographic regions and thus cannot detect unanticipated spatial patterns. We developed a new, data-driven method that uses the first derivative of the spatial smoothing term of a generalized additive model to identify spatial zones of variation in fish length-at-age. We use simulation testing to evaluate the method across a variety of synthetic, stratified age and length datasets, and then apply it to survey data for Northeast (NE) Pacific sablefish (*Anoplopoma fimbria*). Simulation testing illustrates the robustness of the method across a variety of scenarios related to spatially or temporally stratified length-at-age data, including strict boundaries, overlapping zones and changes at the extreme of the range. Results indicate that length-at-age for NE Pacific sablefish increases with latitude, which is consistent with previous work from the western United States. Model-detected spatial breakpoints corresponded to major oceanographic features, including the northern end of the Southern California Bight and the bifurcation of the North Pacific Current. This method has the potential to improve detection of large-scale patterns in fish growth, and aid in the development of spatiotemporally structured population dynamics models to inform ecosystem-based fisheries management.

University of Washington

School of Aquatic and Fisheries Sciences

1122 NE Boat St

Seattle, WA 98105

02 July, 2019

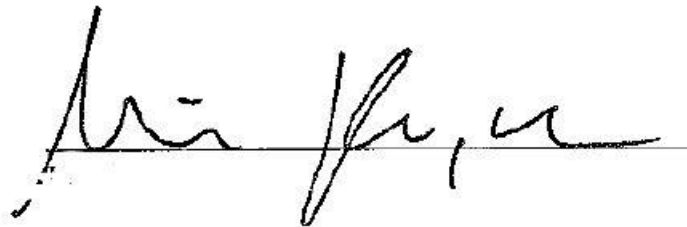
To the editorial board of *Fisheries Research*:

Thank you for the consideration of our paper, *Data driven approach reveals oceanographic features delineate growth zonation in northeast pacific sablefish*. This is a detailed, two-part work that presents a new tool to detect spatiotemporal breakpoints in fish size-at-age, which is then applied to length data from fishery-independent surveys of the valuable sablefish fishery from Alaska to southern California. The case study demonstrates that regions between which sablefish growth differs most can be described by major oceanographic currents, which suggests further impetus towards ecosystem-based management of such stocks. Finally, we anticipate that the tool will be useful for other fisheries scientists seeking a computationally minimal means of detecting changes in growth trends. To that end, we plan to incorporate edits from this peer-review process into an open source R package that readers can use on their own length datasets.

On behalf of my coauthors and myself, we appreciate your consideration of our work and look forward to your feedback.

Best

Maia Sosa Kapur

A handwritten signature in black ink, appearing to read 'Maia Sosa Kapur', written over a horizontal line.

kapurm@uw.edu

Data driven approach reveals oceanographic features delineate growth zonation in northeast pacific sablefish

Kapur, M.¹, Haltuch, M.², Connors, B.³, Rogers, L.⁴, Berger, A.², Koontz, E.⁵, Cope, J.², Echave, K.⁶, Fenske, K.⁶, Hanselman, D.⁶, Punt, A.E.¹

¹ University of Washington, School of Aquatic and Fisheries Sciences. 1122 NE Boat St, Seattle WA 98105

² Fisheries Resource and Monitoring Division, Northwest Fisheries Science Center, National Marine Fisheries Service National Oceanic and Atmospheric Administration. 2725 Montlake Blvd. E. Seattle, WA 98112

³ Institute of Ocean Sciences, Fisheries and Oceans Canada. 9860 W. Saanich Rd. Sidney, B.C. Canada V8L 5T5

⁴ Fisheries and Oceans Canada, School of Resource and Environmental Management, Simon Fraser University. 8888 University Drive, Burnaby, British Columbia, Canada, V5A 1S6

⁵ Center for Quantitative Science, Ocean Teaching Building, Suite 300, Box 357941, Seattle, WA 98195.

⁶ Auke Bay Laboratories, Alaska Fisheries Science Center, National Marine Fisheries Service National Oceanic and Atmospheric Administration. 17101 Pt. Lena Loop Rd. Juneau, AK 99801

Corresponding author: kapurm@uw.edu

Keywords: growth, von Bertalanffy, ecosystem-based fisheries management, sablefish, spatiotemporal

Abstract

Renewed interest in the estimation of spatial and temporal variation in fish traits, such as body size, is a result of computing advances and the development of spatially-explicit management frameworks. However, many attempts to quantify spatial structure or the distribution of traits utilize *a priori* approaches, which involve pre-designated geographic regions and thus cannot detect unanticipated spatial patterns. We developed a new, data-driven method that uses the first derivative of the spatial smoothing term of a generalized additive model to identify spatial zones of variation in fish length-at-age. We use simulation testing to evaluate the method across a variety of synthetic, stratified age and length datasets, and then apply it to survey data for Northeast (NE) Pacific sablefish (*Anoplopoma fimbria*). Simulation testing illustrates the robustness of the method across a variety of scenarios related to spatially or temporally stratified length-at-age data, including strict boundaries, overlapping zones and changes at the extreme of the range. Results indicate that length-at-age for NE Pacific sablefish increases with latitude, which is consistent with previous work from the western United States. Model-detected spatial breakpoints corresponded to major oceanographic features, including the northern end of the Southern California Bight and the bifurcation of the North Pacific Current. This method has the potential to improve detection of large-scale patterns in fish growth, and aid in the development of spatiotemporally structured population dynamics models to inform ecosystem-based fisheries management.

1 Introduction

Fish populations can display spatial patterns in their traits that often do not match the scale or boundaries of management (Denson et al., 2017; Punt, 2019). Spatially and temporally explicit management frameworks promise to reduce decision uncertainty by resolving population heterogeneity (Thorson et al., 2015). Computational limitations long prevented widespread adoption of these tools, but recent advances have driven renewed interest in implementing such frameworks to examine fish population traits (Perretti and Thorson, 2019; Thorson, 2019a). Quantifying spatial and/or temporal variability in fish length-at-age is particularly relevant to understanding demographic variation of this key trait, and can improve the precision of reference points in fisheries stock assessments (Goethel and Berger, 2017; Punt, 2003; Stawitz et al., 2019). Typically, spatial and/or spatiotemporal investigations of variation in fish traits are either exploratory (identifying correlations between traits and environmental phenomena such as temperature, or a proxy for these phenomena, such as latitude [Breitburg et al., 2009; Houde, 1989; Jonassen et al., 2000; Taylor et al., 2018; Trip et al., 2008]) or comparative (determining whether fish traits differ between two or more pre-defined regions or time periods [Adams et al., 2018; Gertseva et al., 2017; Hurst and Abookire, 2006]). We aimed to develop a data-driven method that would simultaneously identify spatiotemporal zones between which fish length-at-age varies, and illustrate correlations between growth and spatiotemporal covariates (such as an increase with latitude). A method to identify such patterns in important population traits can help researchers determine whether current management scales are appropriate given the dynamics present in the population. Because these dynamics are potentially environmentally linked, such a method can also uncover whether spatiotemporal patterns in investigated traits correspond to major environmental features (such as ocean currents) or forcings (such as climatic oscillations), which can help inform the implementation of ecosystem-based fisheries management.

Fish somatic growth rates are typically modelled using the von Bertalanffy growth function (VBGF, von Bertalanffy, 1957) or an alternative functional form, with parameters estimated using model-fitting procedures. The spatial resolution of the resultant estimates is necessarily predicated on the aggregation of the data, which is often defined by survey stratification, political or management boundaries, and/or changes in sampling gear, not necessarily the ecology of the population (McGarvey and Fowler, 2002; Williams et al., 2012). For example, assessments of Alaskan sablefish stocks estimated separate VBGF parameters for two periods of survey data based on the *a priori* hypothesis that changes in survey gear type would affect estimates of fish growth from survey data (Echave et al., 2012; Hanselman et al., 2017; McDevitt, 1990), and imposed a time block between which estimates of the growth curve parameters were quite similar in the stock assessment (see

Table 1). More sophisticated approaches that utilize hierarchical Bayesian methods to estimate latitudinal and regional effects on length- or weight-at-age require a design matrix of

dimensions dictated by pre-supposed zones (e.g. Adams et al., 2018). Such approaches are useful within a management context with rigid spatial boundaries, but do not represent the underlying growth process explicitly, and preclude the discovery of spatially-structured trends in fish size that do not match current management boundaries.

Attempts to quantify spatial variation in somatic growth typically face a trade-off between imposing *a priori* beliefs about stock structure or generating purely descriptive models of trait ‘gradients’ across regions or time periods, without a clear way to identify significant break points within them (King et al., 2001). This presents a gap when developing population dynamics models that accurately represent the structure of managed stocks. The ideal tool is a data-driven method that identifies break points in fish size-at-age, which can then be used to aggregate data and estimate parameters related to somatic growth. To meet this need we present a new method, which uses the first derivative of smooth functions (splines) from a generalized additive model (GAM) to detect change points in spatially- and temporally-structured fisheries growth data that minimizes the use of pre-supposed stratifications in a simple, rapid computational framework. The method does not require the specification of multiple error structures nor the construction of spatial meshes, which can be computationally expensive when large (Thorson, 2019b). The analysis of first derivatives of regression splines in GAMs for change-point analysis has been recently used in terrestrial paleoecology (Simpson, 2018) and geophysics (Beck et al., 2018). The underlying assumption is that the rate of change (the first derivative) of a given predictor is an appropriate measure of the direction and magnitude of the predictor-response relationship. The spline itself may be highly non-linear, but predictor values at which the slope of the spline is largely positive or negative are taken to denote where the response variable is changing the most.

Our method has the potential to improve detection of large-scale patterns in fish growth, and aid in the development of spatially-structured population dynamics models. We use simulation to test the robustness of the method for synthetic length-at-age data of varied complexity, and present a case study application to northeast (NE) Pacific sablefish (*Anoplopoma fimbria*). Sablefish are a highly mobile, long-lived, and valuable groundfish that have high movement rates (10 – 88% annual movement probabilities across Alaska, with a mean great-circle distance of 191 km in a single year; Hanselman et al. 2015) and range from Southern California to the Bering Sea. Concurrent population declines across the entire range over the past few decades have increased concern about the status of sablefish, and interest in identifying the causes of the downward trend. Sablefish stock assessment and management occur independently at regional scales, namely Alaska (AK), British Columbia (BC), and the US West Coast in the California Current (CC), assuming that these are closed stocks. However, recent work has shown that there is little genetic evidence of population differentiation in sablefish across the NE Pacific (Jasonowicz et al., 2017), although there is evidence for differences in growth rate and size-at-maturity throughout the range (McDevitt, 1990). This suggests that the current delineation of assessment and management regions is incongruent with the stock’s actual spatial structure and underscores the potential value of developing a population dynamics model that represents the heterogeneity of sablefish growth throughout their range.

2 Methods

2.1 Method summary

The method fits a GAM to the vector of observed lengths of fish of a single age as the response variable, predicted by separate smoothers at knots t for year, latitude, and longitude, using the mgcv package (Wood, 2011) in R (R Development Core Team, 2011), i.e.

$$g(\mathbf{E}(\mathbf{X})) = \beta_0 + f(y_t) + f(s_t) + f(k_t) + \epsilon_t$$

where $\mathbf{E}(\mathbf{Y})$ represents the expected mean of fish length, g is an invertible, monotonic link function (in this case, the natural logarithm) that enables mapping from the response scale to the scale of the linear predictor, and the additive effects of latitude (s_t), longitude (k_t) and year (y_t), which are smoothed by a thin plate regression spline f . ϵ_t is a residual error term assumed to be normally distributed. The effects of latitude, longitude and year on expected length-at-age are estimated as separate smoothers. To simplify the analysis, we fit the GAM to data for a single age-class and sex at once (e.g., age six for the simulated datasets), thus precluding the need to control for age or sex. Using fish of only a single selected age from all regions also minimizes the concern of differing survey selectivities between regions,

The first derivatives of the linear predictor with respect to latitude, longitude and year are evaluated to identify areas or periods (breakpoints) between which there is evidence for changes in fish length-at-age. The equations below provide an example using latitude s_t , but the process is repeated for each smoother. The finite differences method (as in Simpson, 2018) approximates the first derivative of the trend from the fitted GAM. For instance, the vector of derivatives \mathbf{G} for latitude is produced via the following:

$$\mathbf{G}_t = \frac{g(s'_t) - g(s_t)}{\alpha}$$

where $g(s'_t)$ is a vector of predicted fish lengths at latitudes s'_t , where $s'_t = s_t + \alpha$ and $\alpha = 0.001$ in this analysis, with other effects (year, longitude) held constant. Therefore, the numerators of the elements of \mathbf{G} are predicted lengths at two adjacent latitudes, separated by interval α , which is necessarily small.

The uncertainty in derivative estimates are computed as:

$$SE_t = \sqrt{\mathbf{G}_t \mathbf{V}}$$

where \mathbf{V} is the variance for the current spline; the square root provides the standard error for each derivative estimate of that predictor. These steps are repeated across the range of explored years and longitudes. For each parameter, we identify at which predictor value (e.g., latitude) the maximum absolute value of the first derivative is obtained; this is rounded to the nearest integer and defined as the “breakpoint” if its 95% confidence interval does not include zero. The rounding step was implemented to ease comparison in the simulation study; we did not wish to treat a breakpoint estimate as incorrect if it differed by less than half of one degree (approximately 33 miles) from the true breakpoint. Figure 1 and 2 illustrate the raw data,

smoothers and first derivatives thereof for two synthetic datasets. Once identified, the raw length and age data (including all ages of fish) are re-aggregated based on the identified breakpoints. For each of these new aggregated data sets, the parameters of the VGBF (Equation 4; L_∞ - asymptotic length, k - the rate at which asymptotic length is approached and t_0 - the estimated age at length zero) are estimated using maximum likelihood (in this study using Template Model Builder; Kristensen et al., 2016, assuming that the error is normally distributed with zero mean and variance σ).

$$\text{Equation 4 } \bar{L}_a = L_\infty \times (1 - \exp(-k(a - t_0))) + \varepsilon; \quad \varepsilon \sim N(0, \sigma^2)$$

2.2 Simulation testing

2.2.1 Outline and design

We conducted a simulation study to evaluate the performance of the proposed method, based on datasets generated using an individual-based model (IBM, see Supplementary Material for full details). The IBM is capable of simulating individual characteristics by following the life history processes (survival, growth, and reproduction) of individual fish. We simulate spatial variation by generating length-at-age datasets under different growth ‘Regimes’ (defined as distinct L_1 and/or L_2 values, leading to varied L_∞) and assign latitudes and longitudes to fish grown under each regime. The IBM implements the VBGF using Schnute’s (1981) formulation, which requires k , L_1 , and L_2 , with L_∞ computed as:

$$\text{Equation 5 } L_\infty = L_1 + \frac{(L_2 - L_1)}{1 - \exp(-k \times (a_2 - a_1))}$$

where L_1, L_2 represent the expected lengths of fish at ages a_1, a_2 , and k is the growth coefficient. Each annual increment for every individual fish is subject to bias-corrected lognormal error. We considered five growth scenarios consisting of two growth “Regimes” with either completely distinct spatial or temporal ranges, or spatial ranges with some overlap. We designed our growth regimes to mimic the level of variation in L_1 and L_2 present in the sablefish dataset, which was as high as 26%. In our synthetic population for regime 1 $L_1 = 62$ cm, $L_2 = 215$ cm and $k = 0.25$ yr⁻¹; regime 2 was designed using L_1 and L_2 parameters 20% higher than regime 1 ($L_1 = 74$ cm, and $L_2 = 258$ cm, $k = 0.25$ yr⁻¹). Expected growth curves for the simulated Regimes are present in Supplementary Figure A1.

The simulated spatial extent ranges from 0° to 50° in latitude and longitude. The simulation scenarios (Table 2) were designed to represent a variety of possibilities in spatial growth variation, with one test of the ability to identify a temporal regime change in growth; all simulated datasets were fit using link function g with smoothing functions f for both spatial covariates as well as for year. To simulate spatial zones, locations of fish grown under a certain regime were sampled from a uniform distribution with boundaries defined by the spatio-temporal scenario at hand (see Figure 3). All fish in scenario 1 (no spatial or temporal variation) were grown under regime 1 with latitude and longitude sampled uniformly from 0° to 50°. In scenario 2, the latitude and longitude of fish grown under regime 1 were sampled independently and at random from a uniform distribution between 0° and 25°; fish grown under regime 2 had latitude

and longitude sampled uniformly from 25° to 50°. The same approach was applied for scenario 3, with the change that fish grown under regime 2 had latitude and longitude sampled uniformly from 20° to 50°, thus creating an overlap zone between 20° and 25°. All simulated fish in scenario 4, were assigned latitudes sampled independently and at random from a uniform distribution from 0° to 50°. Fish simulated under regime 1 were assigned longitudes sampled randomly from 0° to 48° and fish simulated under regime 2 have longitudes sampled randomly from 48° to 50°, forming a vertical “band” of larger fish in higher longitudes.

The final simulation scenario (5) involved temporal changes in growth, with a change from growth regime 1 to regime 2 in year 50. This meant that the growth increment generally increased for individuals whose lifespan covers this breakpoint, though note that the GAM is fit to fish of a fixed age. Fish locations for the temporal break scenario are sampled identically to the scenario without spatial variation. Under each scenario, we generated 100 replicate datasets, which averaged 530 age-six fish per dataset (we performed a sensitivity analysis to reducing the sample size by 25% or 50%). For all runs, the initial values for the parameters were $t_0 = 0.1$, $\log(\sigma) = 0.1$, with $L_\infty = 150\text{cm}$ and $k = 0.1$. The estimation procedure also calculated the predicted length at the endpoints of the estimated growth curve (Equation 5; the length at pre-specified minimum (L_1) and maximum (L_2) ages, which were 0 and 15 years in the simulation studies). These values and their standard errors were used in the evaluation of the method (see Section 2.2.2 Performance metrics), as L_∞ and k are typically negatively correlated.

2.2.2 Performance metrics

We considered two performance metrics: 1) the proportion of simulations in which the correct spatial and/or temporal breakpoints were detected - we tabulated the number of times a breakpoint found using a GAM fit to a dataset matched the true latitude, longitude, and year; and 2) the coverage probabilities (determined by the 95% confidence interval) for L_1 and L_2 . For all but the scenario with overlapping ranges (scenario 3), we only considered the GAM analysis to have correctly identified the true breakpoint only if it was an exact match. The ‘true’ dataset for scenario 3 contained fish grown under regimes 1 and 2 in a shared region between 20° and 25° latitude and longitude, so the detected breakpoint was counted as an accurate match if it fell within this range.

For each scenario, after aggregating each of the 100 simulated datasets into the GAM-designated spatiotemporal strata and estimating the growth curve, we determined whether the 95% confidence intervals of the estimated fish lengths at ages zero and fifteen (our a_1 and a_2) contained the true L_1 and L_2 values. For example, fish generated under regime 1 and occupying latitudes and longitudes between 0° and 25° may have been re-aggregated via the GAM analysis into a *de facto* ‘region’ ranging from 0° to 24° degrees for an “early” period of years 1 through 37; the parameters of the VBGF were estimated on this per-strata basis, and the terminal lengths of the estimated curve compared to those from which they were generated, in this case, regime 1. Fits from the complementary *de facto* ‘region’ ranging from 24° to 50°, and/or a “late” period, would be compared to whichever regime generated the majority of fish therein. An estimated

endpoint from a GAM-defined region was considered a match if the 95% confidence interval for it contained the true value of L_1 or L_2 .

To facilitate comparison between the proposed method and an extant approach, we applied the sequential t-test analysis of regime shifts (STARS, Rodionov, 2004) in length-at-age for age 6 to our simulated datasets for both spatial and temporal changes. The STARS method was originally developed to detect climate regime shifts in time-series data, and was noted for its sensitivity to changes towards the end of a series. The method examines the sequential differences in the value of a t-distributed variable, and determines whether subsequent measurements (at the next year or latitude, for example) exceed the expected range. We used a minimum regime ‘length’ of five, meaning detected shifts between latitudes, longitudes or years must persist for at least five consecutive units, and the default p-value cutoff of 0.05. We believe this captures the timescale of regime shifts of interest to ecologists, and a significance cutoff frequently used in such analyses. From the STARS analysis of each dataset, we selected the breakpoint(s) with the largest positive “regime shift index”, which represents a cumulative sum of the normalized anomalies. This is qualitatively similar to the “largest first derivative” metric used in the proposed method and, as in that case, was applied regardless of where the breakpoint was detected. We implemented the same steps, whereby the detected spatial and/or temporal breakpoint(s) were used to re-aggregate and estimate growth parameters, and the proportion of accuracy and coverage probabilities for L_1 , and L_2 tabulated.

2.4 Application to Northeast Pacific Sablefish

We obtained fishery-independent length and age data from the Bering Sea, Aleutian Islands, and Gulf of Alaska Sablefish Longline Survey (Rutecki et al., 2016) and the U.S. West Coast Groundfish Bottom Trawl Survey (Northwest Fisheries Science Center, 2019) conducted annually by the Alaska Fisheries Science Center and the Northwest Fisheries Science Center, respectively. We also obtained length and age records from the Canadian Department of Fisheries and Oceans (Wyeth et al., 2005); see

Table 1 for a summary of survey data used in the application. Data from each region included measured length, sex, age, and the starting latitude and longitude, which determined the survey station. Due to computational constraints, and to avoid disproportionate influence of more heavily-sampled regions on breakpoint estimates, we randomly subsampled 15,000 total records from each of the three management regions. The subsampling was random with respect to latitude, longitude, age and sex, using the `sample_n` function from the package *dplyr* (Wickham et al., 2019).

We applied the method to identify spatial and temporal breakpoints for each sex separately at several key ages: age 4 (before length-at-50%-maturity for both males and females in all regions), age 6 (after length-at-50%-maturity for both males and females in all regions) and age 30, roughly the length at which sablefish are expected to obtain their maximum length (Johnson et al., 2015). Our sampling method produced a data set with an average of 1,315 age 4, 1,283 age 6, and 65 age 30 sablefish of each sex from each region. Growth model fitting was performed

using all available data from each of the three management regions (see Supplementary Table A3 for sample sizes).

In constructing the GAM, we investigated the use of an AR1 temporal structure for the residual ϵ_t with lags of 1 to 3 years, but these models did not improve AICc over the initial model (without autoregressive structure). We re-aggregated all data to match the breakpoints that appeared in the GAM analysis for key ages, as well as an ecosystem-based breakpoint at 145°W. We selected this breakpoint based on work by Waite and Mueter (2013) who used cluster analysis to delineate unique regions of chlorophyll-*a* variability, which has been shown to be influential in the sablefish recruitment process (Shotwell et al., 2014) but by definition such an effect is not detectable in our analysis that only examines fish larger and/or older than recruits. The North Pacific Fishery Management Council uses 145°W, which includes a cluster of several seamounts in the Gulf of Alaska, to delineate a groundfish slope habitat conservation area (Siddon and Zador, 2018). We employed a stepwise exploration of whether estimates of L_∞ were significantly different between regions detected using the method and generated from this ecosystem break using the entire, non-sub-sampled dataset. This involved first aggregating and estimating the VBGF for ten unique spatiotemporal strata for each sex, defined by the three spatial and one temporal breakpoints found among the key ages selected for analysis using the GAM in addition to the break at the aforementioned ecosystem feature. We then examined whether the 95% confidence intervals for L_∞ overlapped for any temporally-split datasets from the same region (e.g., region 1 female sablefish data before and during 2010 and after 2010). If they did, we pooled the data for that region and sex for all years. In the second step, we examined if spatially-adjacent regions (from any time period) for the same sex had 95% confidence intervals for L_∞ that overlapped, and combined regions for which this was the case on a by-sex basis. This stepwise approach reduces unnecessary partitioning of the data into spatiotemporal strata that do not ultimately result in different estimates of L_∞ , and allowed us to examine whether any of our detected breakpoints or the *post hoc* ecosystem split was informative regarding growth estimates. Once the most parsimonious structure was identified through this method, we generated predicted lengths-at-age for the entire dataset.

3 Results

3.1 Simulation Study

The simulation study demonstrated that the first-derivative GAM-based method is able to detect both spatial and temporal breakpoints correctly in the majority of scenarios, with the exception a scenario where the spatial break occurred near the edge of the study region at 48° longitude, where it only detected the break location correctly in 15% of simulations. Figure 4 displays the coverage probabilities for the 95% confidence intervals and proportion of simulations wherein the correct breakpoint was detected. Supplementary Figure A2 presents a histogram of detected breaks for each scenario.

For all scenarios, the method achieved the highest coverage probabilities for the length-at-age 0 (L_1) [32%-69% coverage for three scenarios and 24% in the scenario with overlap].

Coverage probabilities for length-at-age 15 (L_2) were lower [4% - 17% for three scenarios and 7% in the scenario with overlap]. In terms of spatial breakpoint detection, there was not a qualitatively strong difference in the method's ability to correctly detect latitudinal vs. longitudinal breakpoints across scenarios. Our method correctly detected the lack of a breakpoint in over 90% of simulations without breaks; there was no discernable pattern to the spurious spatial breakpoints identified in the remaining simulations. The method did less well at detecting the accurate breakpoints for scenario 4 (a "true" spatial break at 48°), assigning the break between 46° and 50° longitude in 100% of simulations; similarly, for the scenario with a single breakpoint at 25°, 100% of mis-detected breakpoints were incorrect by a single degree (assigning latitude and/or longitude to be 24° or 26°). The method achieved 75%-87% accuracy in correctly detecting no temporal breakpoints in scenarios where it was absent. Though the method only detected the correct temporal break (year 50) in 63% of time-varying simulations, 89% of the remaining simulations assigned the break to year 49 or 51, increasing the total detection between years 49, 50 and 51 to 96%. We computed the absolute error between the end of the estimated 95% confidence interval and the true parameter for simulations which 'missed' (did not contain) the true value for each scenario. If the true parameter value was higher than the confidence interval, the difference was measured from the upper end of the interval, and vice versa. The maximum error in both L_1 and L_2 was obtained for Scenario 2 (single breakpoint at 25°) at 8.89 cm and 22.7 cm, with the minimums obtained by Scenario 1 at 0.04 cm and 0.32cm. There was no discernable pattern to the spurious years assigned to scenarios without actual temporal variability. We did not find the method's accuracy or resultant coverage probabilities sensitive to either halving or reducing the sample size by 25%; see Supplementary Table A2.

3.2 Comparison to STARS Method

The STARS method (Supplementary Figure A15) was inferior to the proposed GAM-based method at detecting spatial or temporal break points for all simulated scenarios, with a slight exception for the break at edge case (scenario 4). In that scenario, the STARS method was able to detect the correct longitudinal break in 31% of datasets. For all other scenarios, it averaged 14% accuracy in detecting latitude, 13% accuracy in detecting longitude, and 64% accuracy for year breaks (compared to 95%, 96% and 77%, respectively, for the GAM-based method). However, it performed comparably in terms of the coverage probability of L_1 (51% vs 47% for the GAM-based method) and better in terms of coverage probability for L_2 (32% vs 7%).

3.3 Application to NE Pacific Sablefish

The latitude smoother suggested a generally increasing cline in length-at-age with latitude, with a significant breakpoint around 50°N (approximately the northern end of Vancouver Island, Canada) detected when the GAM was fit for age four and six sablefish (Figure 5c, 6c; Supplementary Figures A4, A7). Above this breakpoint, female L_2 estimates were consistently larger than 70 cm, whereas they were consistently smaller than 66 cm south of it. Both age six and age 30 female sablefish identified a breakpoint at 36°N (approximately Monterey, CA,

USA). Both males and females obtained the lowest estimated L_2 south of this breakpoint, at 55 cm for males and 60.43 cm for females. In all regions, L_∞ was higher for female sablefish than males, and the resultant L_2 differed between regions within sexes by up to 26%. The temporal smoother did not exhibit a strong one-way trend, and was flat for age-30 fish of both sexes, though it did detect a break in 2009-2010 for both sexes of age 4 and 6 sablefish. Parameter estimation for this initial stratification according to our breakpoints revealed that the 95% confidence intervals for L_∞ between time periods overlapped for males within all regions and for females in regions 3, 4 and 5 (Supplementary Figure A12). The number of spatiotemporal strata was reduced to 13 after combining years of data for region-sex combinations where overlap was found in the second phase. Once re-aggregated and re-estimated, we did not find overlapping confidence intervals for L_∞ for any adjacent regions (Supplementary Figure A14), so this set of specifications was retained as our final spatiotemporal stratification. The stratification consists of three regions bounded on their western border by a break at 130°W; from south to north, these regions (labeled 1, 2 and 3 on Figure 7) are defined by latitudes 36°N and 50°N. These breaks correspond generally to Monterey, CA and the northern tip of Vancouver Island, BC. Region 4 is the area between 130°W and the ecosystem break at 145°W (roughly Cordova, AK). Datapoints collected to the west of the ecosystem break are assigned to Region 5.

4 Discussion

We determined that the proposed, GAM-based method was able to accurately detect spatial and temporal breakpoints more frequently than the STARS method, with the exception of breakpoints occurring at the edge of the study region. For NE Pacific sablefish, we applied the method to each sex separately at a set of key biological ages and determined that sablefish length-at-age differs most significantly across five regions, whose boundaries can be defined by major oceanographic features (the Southern California Bight, and the bifurcation of the North Pacific Current) as well as a known ecosystem boundary in the Gulf of Alaska. Below, we discuss the results of the simulation study and provide further guidance on how researchers could apply our proposed method to new datasets. We then discuss the results found during the application to northeast Pacific sablefish, with respect to ecosystem concerns.

4.1 Implications of Simulation Results

The method performed best for both performance metrics for the scenario in which growth regimes 1 and 2 overlapped (which had the advantage of being ‘matched’ whenever the breakpoint fell within 20° to 25°). The most commonly detected breakpoint in latitude and longitude for that scenario, before rounding, was the midpoint of this range (22.5°), likely an artifact of the penalization function within the GAM, which seeks to minimize curvature on either side of a given knot (i.e., the breakpoint). This penalization function controls the degree of smoothness on the spline and can lead to fitting overly-complex models when unchecked (Wood, 2003). Since the purpose of this analysis was diagnostic (the detection of where the spline is changing the most), we were able to avoid undue influence from this parameter by a) selecting only the value corresponding to the maximum first derivative and b) that had confidence

intervals not containing zero, which are common in highly curved splines. This did not preclude detection of spurious spatial or temporal breaks in ~10% of simulations for which no breakpoints were present. However, some erroneous detection can be expected considering the inherent noise in our datasets, and that there is no minimum threshold for breakpoint detection; a single, small derivative among many zeros that did not have a confidence interval containing zero could be ‘picked’. This observation partially motivated the two-phase procedure employed for the sablefish application, so it is likely that such erroneous detection would be reduced if overlapping growth estimates were disregarded (our simulation analysis investigated the accuracy of the first stage). We evaluated if an autoregressive structure improved our models as length-at-age can be time-dependent but it did not; this may not be the case for other fisheries.

The procedure for deciding whether the method was accurate was inherently strict, in that simulations were determined inaccurate if the detected breakpoint was in error by only one degree (approximately 110 km). As presented in Section 3.1 Simulation Study, these near-misses characterized 100% of detections in the scenario with a single breakpoint in space or time; relaxing the matching criteria to include neighboring points would increase the performance by allowing a greater range of detected breakpoints to be counted as ‘correct’. The good performance of the method despite this strictness is promising. In addition, we did not simulate nor consider error or bias in the aging (i.e., otolith reading) process (Cope and Punt, 2007), which would potentially introduce uncertainty in breakpoint detection. With these caveats in mind, we envision (and demonstrate) using the method as a tool to identify general regions and periods of change in fish length-at-age, which will necessarily be evaluated against pre-existing knowledge of the fish population and its ecosystem.

We observed decreased ability of the method to detect breakpoints near the edge of the range, with a true break at 48° inconsistently being assigned between 46° and 50°. This outcome, and the resultant low coverage probabilities for parameters L_1 and L_2 for this scenario were likely due to the smaller number of samples present in the ‘edge’ region, and contrast in length-at-age between the two regions, which rendered estimates of aggregated data uninformative. This suggests that fishery scientists and managers may need alternative tools to detect and appropriately consider variation in growth at the extremes of a stock’s spatial domain, or occurring at present. Such breakdown of detection methods at the margins of a series (at the edges of a study region, or at the end of a time-series) has been documented in Rodionov (2004), who developed a method using sequential t-tests (STARS) to perform edge-case detection, and applied it to detect ecosystem regime shifts in the Bering Sea (Rodionov and Overland, 2005). The t-test approach can be tuned by the researcher to control the level of significance that determines a regime shift (or breakpoint), presenting the same challenge of spurious and/or missed detections depending on the sensitivity of the statistical test applied. Our comparison with the STARS method demonstrated that the GAM-based method performs better at accurately detecting spatial-temporal breakpoints, with the exception of scenarios where the break occurs at the edge of the study system, which was expected. In terms of the coverage probabilities, both methods had a reduced ability to correctly estimate L_2 , with the STARS method performing

slightly better. We believe this outcome is due to two interacting processes: the GAM-based method's sensitivity to temporal variation, and bias in parameter estimates due to reduced sample sizes at high ages. The GAM appeared to be more sensitive to temporal signals in the datasets, and though it correctly detected (or correctly failed to detect) a temporal breakpoint in the majority of datasets, when it mis-detected a year break it did so seemingly at random, thus splitting the dataset into arbitrary groups and leading to lower accuracy of estimation. This phenomenon was more pronounced for L_2 since L_2 relies on fish near the terminal age, of which there are typically fewer, and can lead to bias in the resultant estimate when the already-small sample of fish at age a_2 is split further due to spurious year detections. Indeed, for all scenarios besides Scenarios 1 and 4 (no breaks and break-at-edge), the margin by which L_2 was missed was greater in simulations that mis-detected the year break (see Supplementary Material, Table A4). For assessment methods that estimate VBGF growth parameters within the assessment model, this low-data/low-accuracy issue for the terminal length may induce greater uncertainty (e.g., the need for priors with lower standard deviations) until targeted survey sampling can improve precision in less-represented regions.

It is also relevant that neither the GAM-based nor the STARS approach is appropriate for extrapolation (prediction beyond the range of covariates, or outside of the ecosystem, used in model fitting), particularly because they use indirect variables such as latitude which may have nonlinear or inverted relationships with fish physiology in other regions (Austin, 2002). It is likely there are thresholds in, or types of, spatiotemporal growth variation that will be poorly detected by most methods, which we see as a promising area for future research, although we did not account for or simulate error or bias introduced from errors in assigned ages to animals.

Empirical work has suggested that somatic growth in fisheries follows ecosystem gradients rather than management boundaries (Pörtner and Knust, 2007; Taylor et al., 2018). The ongoing emphasis on ecosystem-based fisheries management calls for the analysis of fish stocks at meaningful spatial scales, across which changes can be detected. Absent an ecosystem-wide analysis, strong directional trends in any generalized additive term (such as the positive trend with latitude observed here) or a breakpoint at the edge of the study region can be indicative of a change somewhere in the margins and extend the reach of future survey designs.

Our method indicated tradeoffs between the accuracy of breakpoint detection and resultant coverage probabilities in the estimated growth curve, as well as large differences in the coverage probabilities of fish length at younger versus older ages. We find it encouraging that the approach could correctly detect breakpoints for the scenario with overlapping ranges, which is likely more similar to real-world fish populations than the singular, immediate breakpoints simulated in other scenarios. However, the assigned 'zonation' of these populations necessarily combined fish with contrasting growth curves into a single dataset for estimation, and resulted in a loss in accuracy (coverage probability) for the endpoints of the growth curve. We suggest the method be used as a tool to guide the identification of general zones between which growth could vary, and not take detected breakpoints as the absolute truth. Importantly, suggestions of spatial breakpoints produced by the method should necessarily be considered in the context of

the ecosystem, and prior knowledge of how the fishery at hand responds to features (e.g., temperature, depth) which vary with latitude and/or longitude.

4.2 Northeast Pacific Sablefish

Our evaluation of size-at-age for NE Pacific sablefish was directly motivated by the notion that sablefish growth may vary at a scale that differs from present management boundaries. Estimates of the growth parameters for sablefish are usually based on survey data acquired from chartered commercial trap, trawl or longline vessels (Table 3). It is preferable to obtain estimated growth parameters from data collected using a survey, because fishery-dependent information can be systematically biased due to targeting or gear selectivity (Ricker, 1969). It is curious that the model identified a unique spatial zone (region 3; Figure 7) comprised exclusively of sablefish sampled in British Columbia (though not all BC data were encompassed by region 3). As anticipated, L_{∞} estimated for this region for each sex was distinct from that for adjacent zones, but it is possible that the trap-based survey method, unique to BC, exhibits length-based selectivity currently unknown to (and not reflected in) in the current assessment (Department of Fisheries and Oceans, 2016), which then gives rise to this result. Selectivity, if determined, can be corrected for via a truncation in the normal distribution for fish obtained in that region; selectivity is also assumed to be equal to one for all lengths in both the AK Federal (Hanselman et al., 2017) and the CC (Johnson et al., 2015) assessments and so no truncation was performed. Researchers interested in using the method presented here are advised to consider carefully how biases in their data may emerge as erroneous breakpoints and resultant growth estimates when interpreting results.

It is evident from this and previous work (Echave et al., 2012; Gertseva et al., 2017; McDevitt, 1990) that there is some level of variation in sablefish growth, whether in the growth rates themselves or the spatiotemporal scale at which variation in growth occurs. Previous work with sablefish data has utilized an *a priori* method, wherein length and age data were aggregated into pre-hypothesized spatial zones and fitted VBGF curves were compared via Akaike's Information Criterion. This 'information-theoretic' (Guthery et al., 2003) method is fairly straightforward computationally, and has been implemented separately for the California Current (Gertseva et al., 2017) and Alaska federal sablefish fisheries (Echave et al., 2012; McDevitt, 1990). The CC analysis identified a statistically significant break in VBGF parameters for sablefish at approximately 36° N, between Point Conception and Monterey, CA, with additional evidence for an increasing cline in L_{∞} with increasing latitude and a general increase in estimated L_{∞} and L_2 for more northerly regions. These results mirror the trend in our latitudinal smoother (Figure 5 and 6) and our detected breakpoint at 36°N (Figure 7), which is incidentally a management sub-boundary used by the US Pacific Fishery Management Council. That work also found an increase in k estimates for areas sampled south of the Vancouver region (ca. 49°N), which was posited to be the result of samples coming from the "southern end of a faster-growing northern stock", a suggestion supported by our findings of another breakpoint at 50°N. Preliminary analyses of sablefish tagged in Alaska suggest that the BC region exports fish into

the CC and Gulf of Alaska, a diffusion pattern that could potentially taper off with decreasing latitude; the distance between Vancouver, B.C. and Monterey, C.A. is approximately three times the mean great-circle distance for sablefish determined by Hanselman et al. (2015). Gertseva et al. (2017) described how sablefish have been shown to be highly mobile, with ontogenetic movements off the coastal shelf; such combined, complex life patterns could yield higher growth rates in northern regions that interact with a more generalized shelf-slope pattern of ontogenetic movement observed in groundfish overall.

For Alaska, a generalized linear model of length as a function of pre-specified zones and time blocks was used to diagnose a ‘regime change’ in sablefish growth occurring in 1995 (Hanselman et al., 2017), though the authors explain this shift is possibly attributable to changes in sampling strategy that occurred in that year’s survey. In the recent AK sablefish assessments, the parameters of the VBGF are time-blocked accordingly (

Table 1) despite caution that the change is not inherent to the population, but likely an artifact of sampling methods. In our analysis (which included data for all regions), the first derivative did not contain zero in 1995 only for age-four fish, although it was not of greater magnitude than the derivative for 2010. This may be indicative of a change in selectivity for age four sablefish, rather than a change in growth.

There are several noteworthy trends in the stratified growth estimates (Figure 8) that warrant future research. Firstly, the *post hoc* incorporation of a spatial break at 145°W based on ecosystem data was not ruled out during the significance testing of L_{∞} . This supports the notion that environmental features may result in variations in growth, and that the proposed method is amenable to improvements based on the incorporation of climate or ecosystem knowledge. In the future, it is conceivable that the method could explicitly incorporate climatic data (such as temperature, or a factor for an ecological zone). Additionally, both latitudinal breakpoints are associated with significant oceanographic features, namely the start of the southern California Bight at Point Conception (~34°N) and the bifurcation of the North Pacific Current, which splits into the Alaska and California currents as it approaches the west coast of North America. The location of this bifurcation varies, but is generally centered off the coast of British Columbia (Cummins and Freeland, 2007; Figure 7). In common with the ecosystem split identified in the Gulf of Alaska, these oceanographic features lead to distinct zones of productivity (Kim et al., 2009; Mackas et al., 2011) that could influence resource availability and subsequent growth.

This finding is especially notable in the context of the countergradient growth variation hypothesis (Levins, 1968). This hypothesis states that two populations may exhibit similar phenotypes (i.e., length-at-age) even if they are genetically predisposed to grow at different rates if their environment modulates growth rate in a direction counter to their predisposition. This effect has been observed empirically in several oceans (Baumann and Conover, 2011; Conover et al., 1990). One of the key species for which the countergradient hypothesis was confirmed was Atlantic silverside, which in common with sablefish participate in ontogenetic migrations on and off the continental shelf. Considering recent genetic evidence that the sablefish population

examined here is genetically well mixed (Jasonowicz et al., 2017), we could expect that observed phenotypic variation is a direct result of such environmental inhibition or enhancement.

It appears that the temporal break in year 2010 was conserved (supported by significantly different L_{∞} estimates) only for female fish, and more so in the southerly regions (such as Regions 1 and 2, which are mostly comprised of CC data). Preliminary analyses of sablefish movement rates from tagging data from Alaska (as analyzed in Hanselman et al., 2015) indicate that male sablefish seem to move more frequently to and from sea mounts, which are clustered within the regions identified here. There are several possibilities for why female sablefish seem to exhibit finer spatiotemporal structure in growth. Older empirical work in Canada (Mason et al., 1983) that examined early life history of fishery-caught coastal sablefish observed a slight cline in mean fork length with increasing latitude, although the sex ratio within the study was biased towards females. That study suggested that selectivity for female sablefish may be higher due to higher congregating or feeding activity, in addition to the fact that females grow larger and are likely preferentially targeted in the commercial fishery in BC, which is also true for the fixed-gear fisheries in the CC (Johnson et al., 2015). This could render females more sensitive to changes in fisher behavior such as the implementation of catch shares off the US west coast in 2011, which affected discard rates in many groundfish fisheries (Somers et al., 2018). Expanding the method to allow for detection of multiple spatial and/or temporal breaks at once may enable further investigation of this phenomenon, although it may lead to spurious regions of insignificant difference in growth parameters, as observed in the first phase of the case study.

Consideration of temporal variation in sablefish growth is further complicated by the exploitation history of the fishery, which has steadily moved north- and west-ward in the CC and AK over the last several decades, encountering ‘larger’ fish with subsequent expansion (Pacific Fisheries Management Council (PFMC), 2013). This suggests that differences in mean length across the region could be attributable to different degrees, durations, or patterns of fishing pressure (Hilborn and Minto-Vera, 2008), interacting with inherent growth variation to produce such spatiotemporal patterns. A principal conclusion of Stawitz et al. (2015) was that the form of sablefish growth variation differed among ecosystems, wherein the CC is a more climactically variable region. Such ecosystem-driven trends may be diluted when analyzing the data as a composite, as in our study; notably, our temporal smoother did not produce a distinct annual or cyclic trend. Methods that consider the space and time components co-dependently (as in vectorized auto-regressive spatiotemporal models, Thorson, 2019a) may strengthen the ability to disentangle such trends, and also to consider covarying spatial effects (e.g. near- and offshore).

4.3 Conclusions

We aimed to develop a method that would identify spatiotemporal zones between which fish growth varies, while simultaneously illustrating directional correlations in growth. The method shows promise for the accurate detection of spatiotemporal breakpoints in fish length-at-age. When applied to NE Pacific sablefish, our method determined that the current management scale (three political breaks at national boundaries) is incongruent with the underlying pattern of variation in sablefish growth. Further research will help determine the impact of this spatial mis-

591 specification on fisheries management reference points. Importantly, we discerned that the
592 spatial variation in sablefish growth can be explained by major oceanographic features,
593 principally the splitting of two major ocean features and the edge of a highly productive zone.
594 This finding supports the impetus towards ecosystem-based fisheries management, and motivates
595 further research into the effects of spatial and/or growth mis-specification on assessment
596 outcomes for sablefish and similar species in the region.

Figures

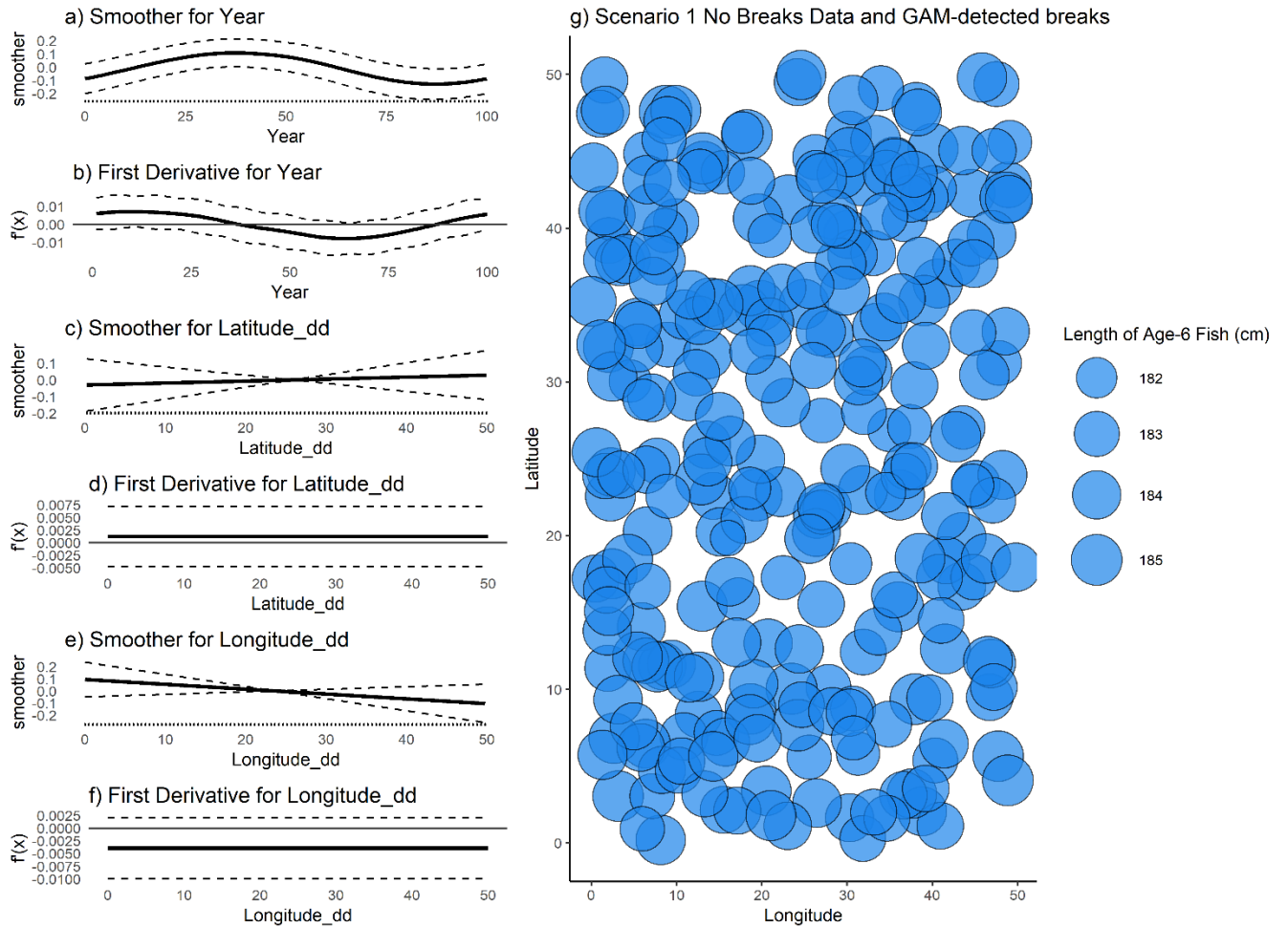


Figure 1. (a,c,e) raw value of GAM smoothers for Year, Latitude and Longitude; (b,d,f) mean (black line) and 95% CI (black dashed lines) of first derivative of the smoothers; (g) map of age-6 fish for a single simulated dataset with no designated spatial or temporal breaks. No break points were detected by the GAM.

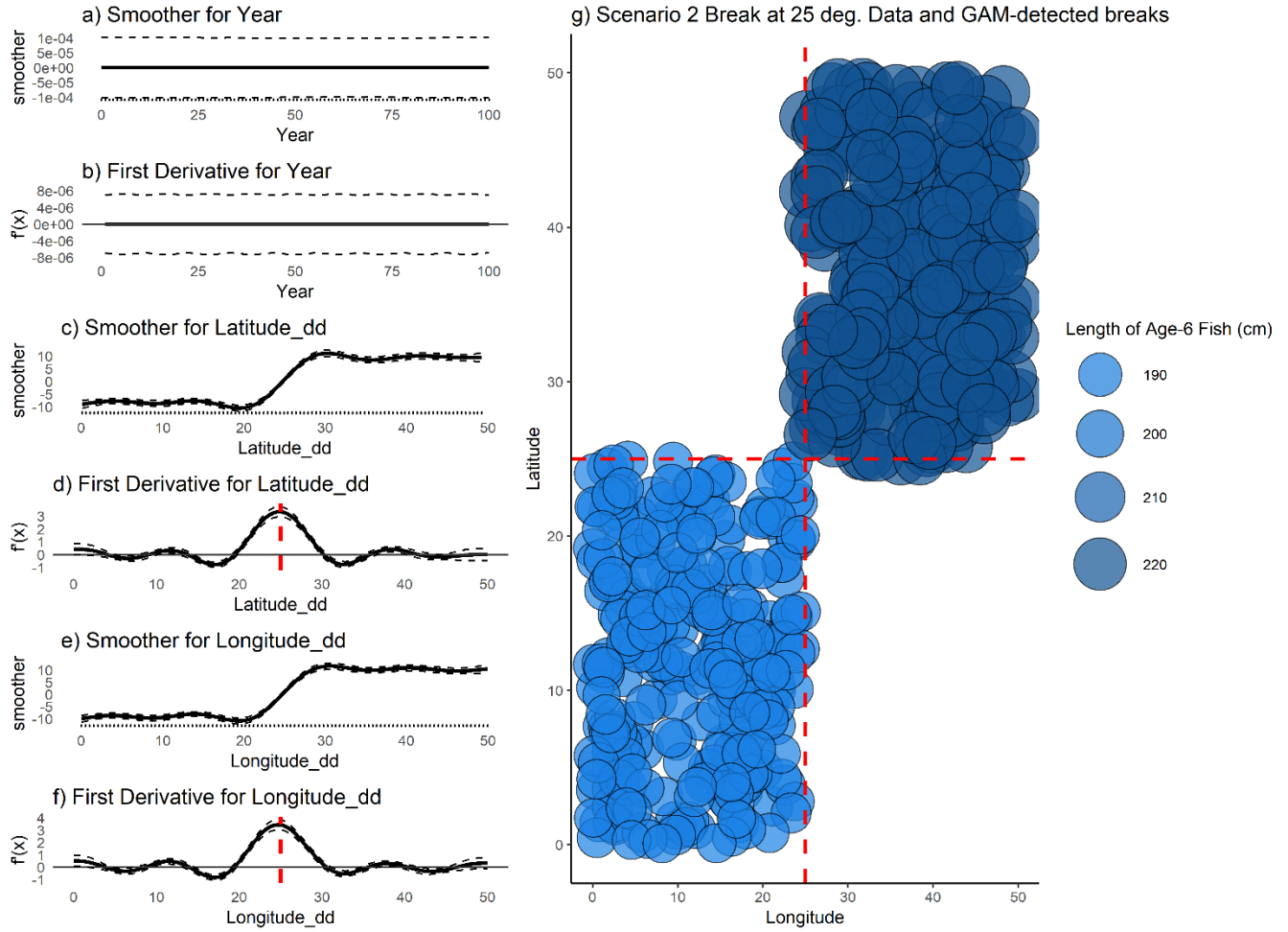


Figure 2. (a,c,e) raw value of smoothers (fitted regression splines) for year, latitude, and longitude; (b,d,f) mean (black line) and 95% CI (black dashed lines) of the first derivatives of the smoothers; (g) map of age-6 fish for a single simulated dataset with a single, symmetrical break at 25° latitude and longitude. Dashed red lines indicate detected break points, which are the maximum value obtained for this data set and do not have a confidence interval that contains zero.

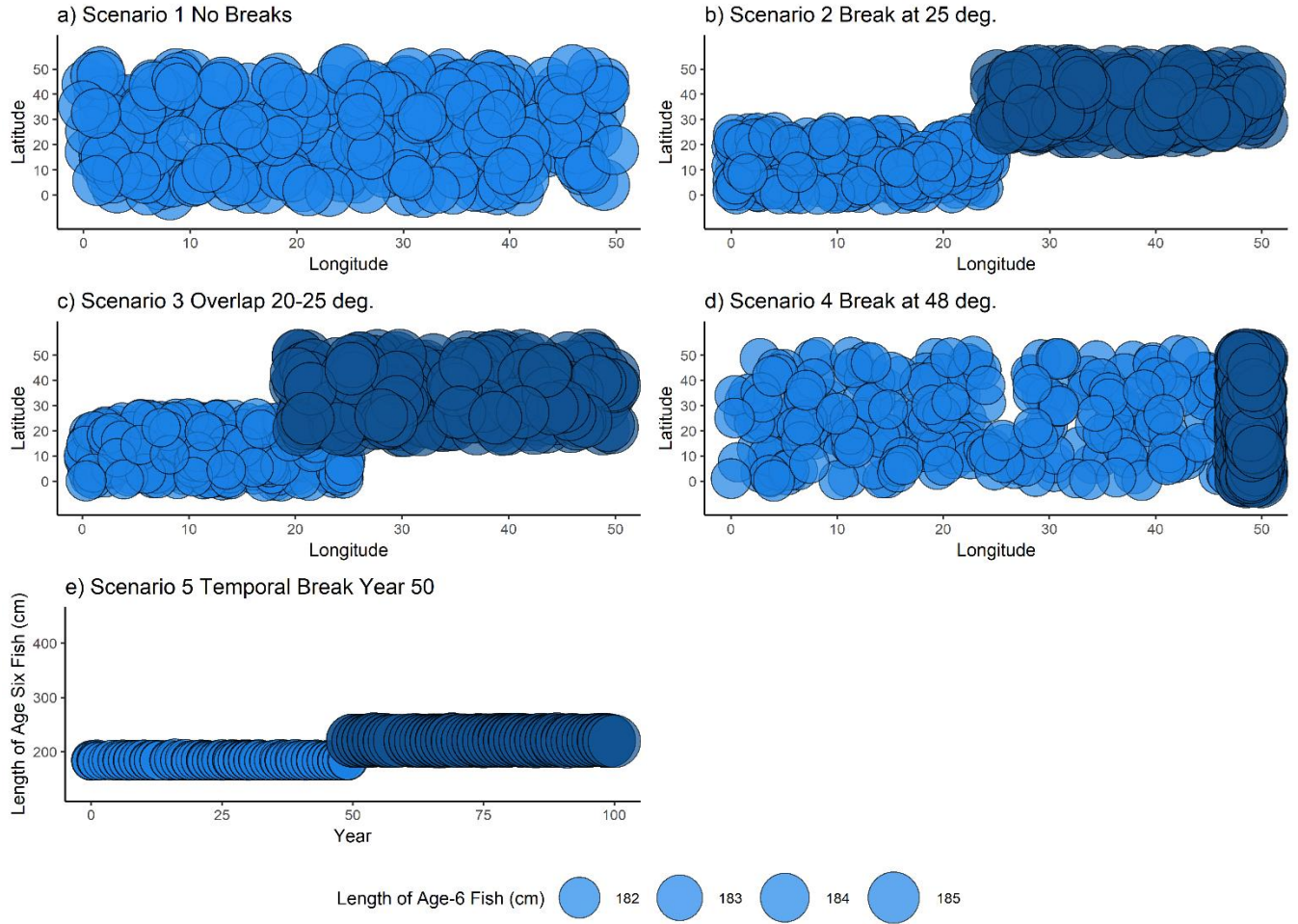


Figure 3. Example dataset for each of the scenarios in Table 2. For each of the five scenarios, points represent the length and location of a single simulated fish at age six. Fish locations (latitudes and longitudes) were sampled from a uniform distribution of the boundaries indicated in Table 2.

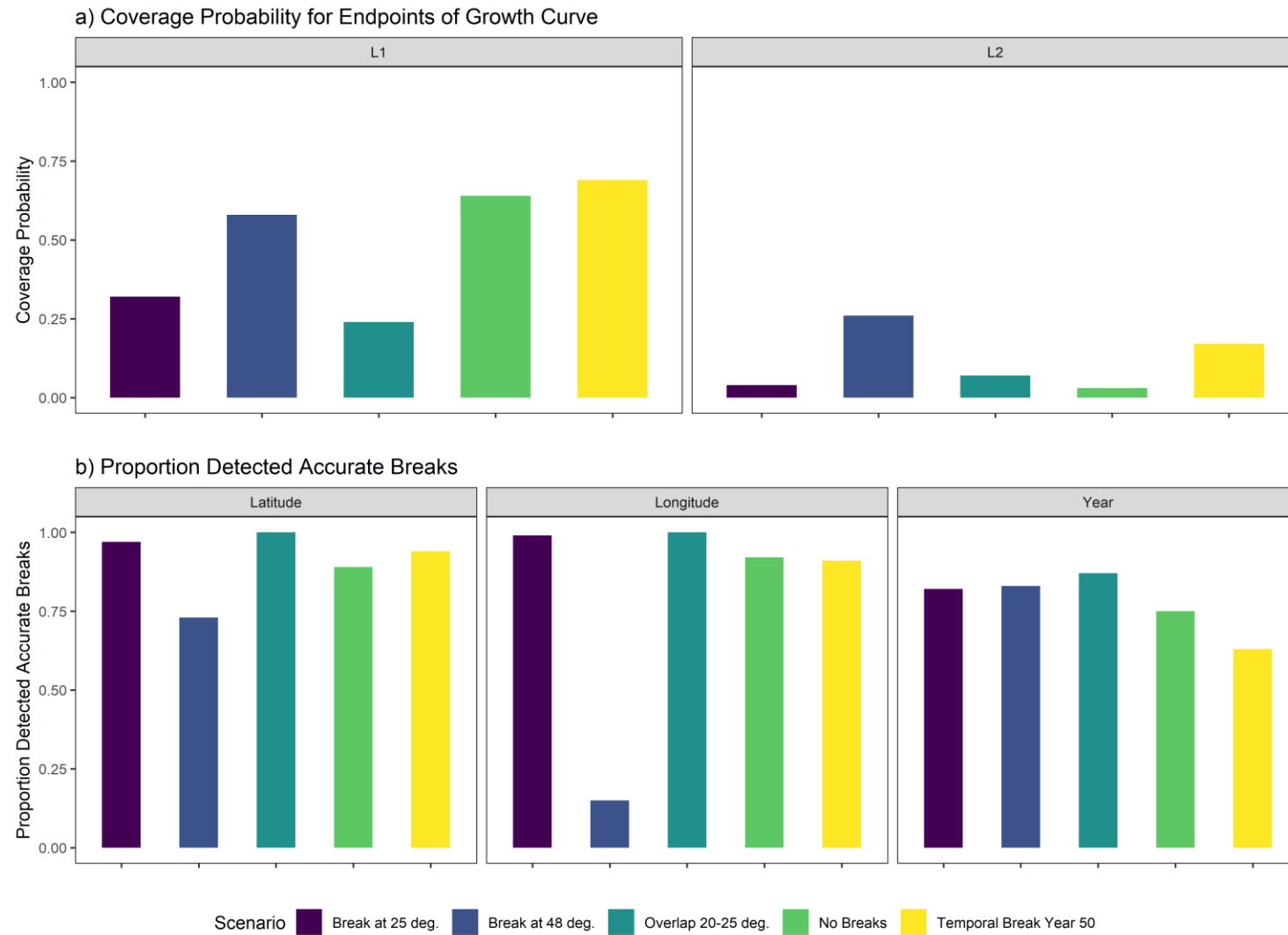


Figure 4. a) coverage probabilities for the endpoints of the growth curve, L_1 (left) and L_2 (right), and b) proportion of 100 simulations for each spatial scenario wherein the correct latitudinal breaks (left), or longitudinal breaks (center) or temporal break (right) were detected.

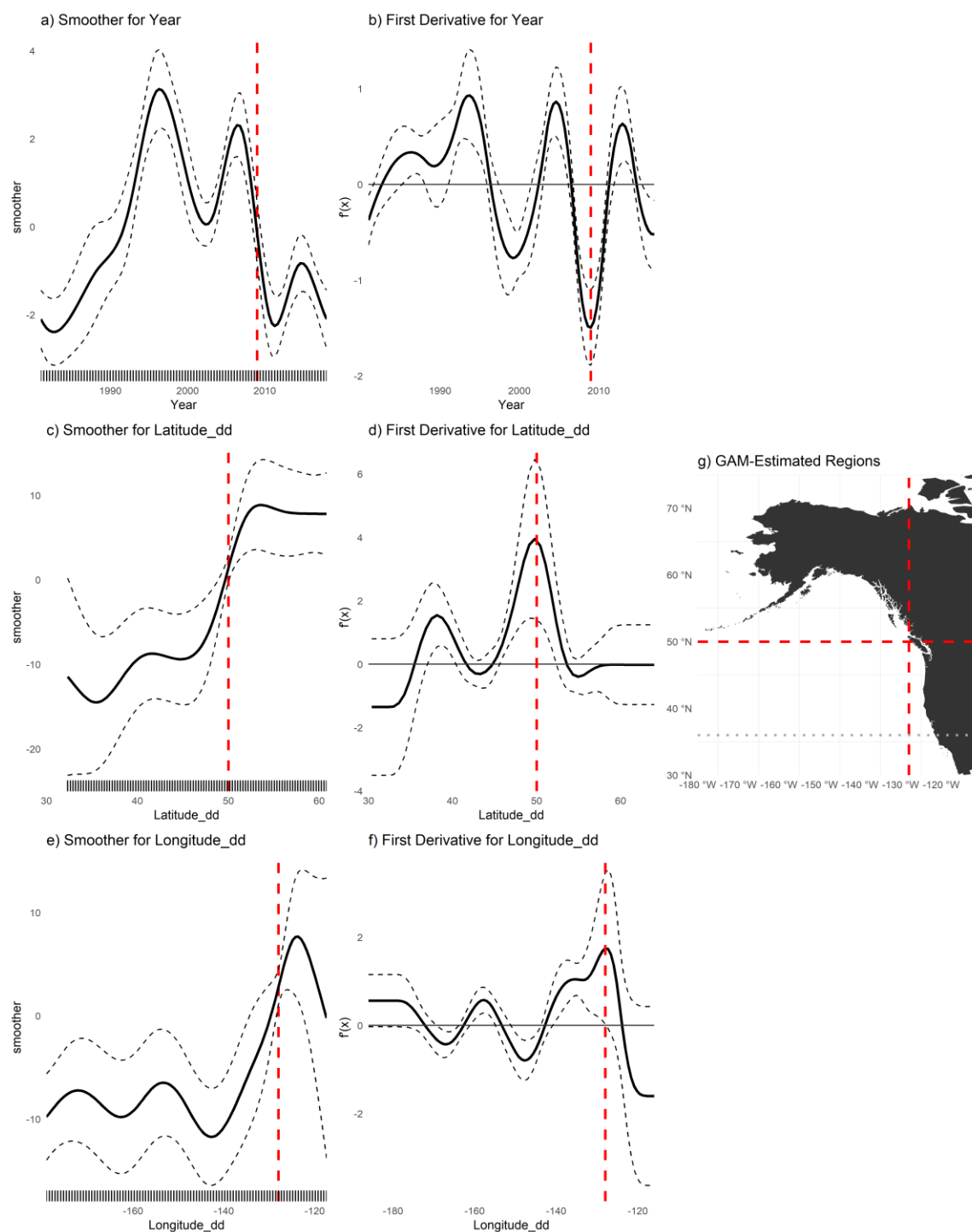


Figure 5. (a,c,e) Plots of smoothers (fitted regression splines) for year, latitude, and longitude, and first derivatives thereof for female age four sablefish (b,d,f). On a-f, vertical dashed lines indicate latitudes, longitudes or years that correspond to the highest first derivative and had a confidence interval that did not include zero. g) map with model-detected breakpoints (red dashed lines) and breakpoints detected for other ages (grey dotted line).

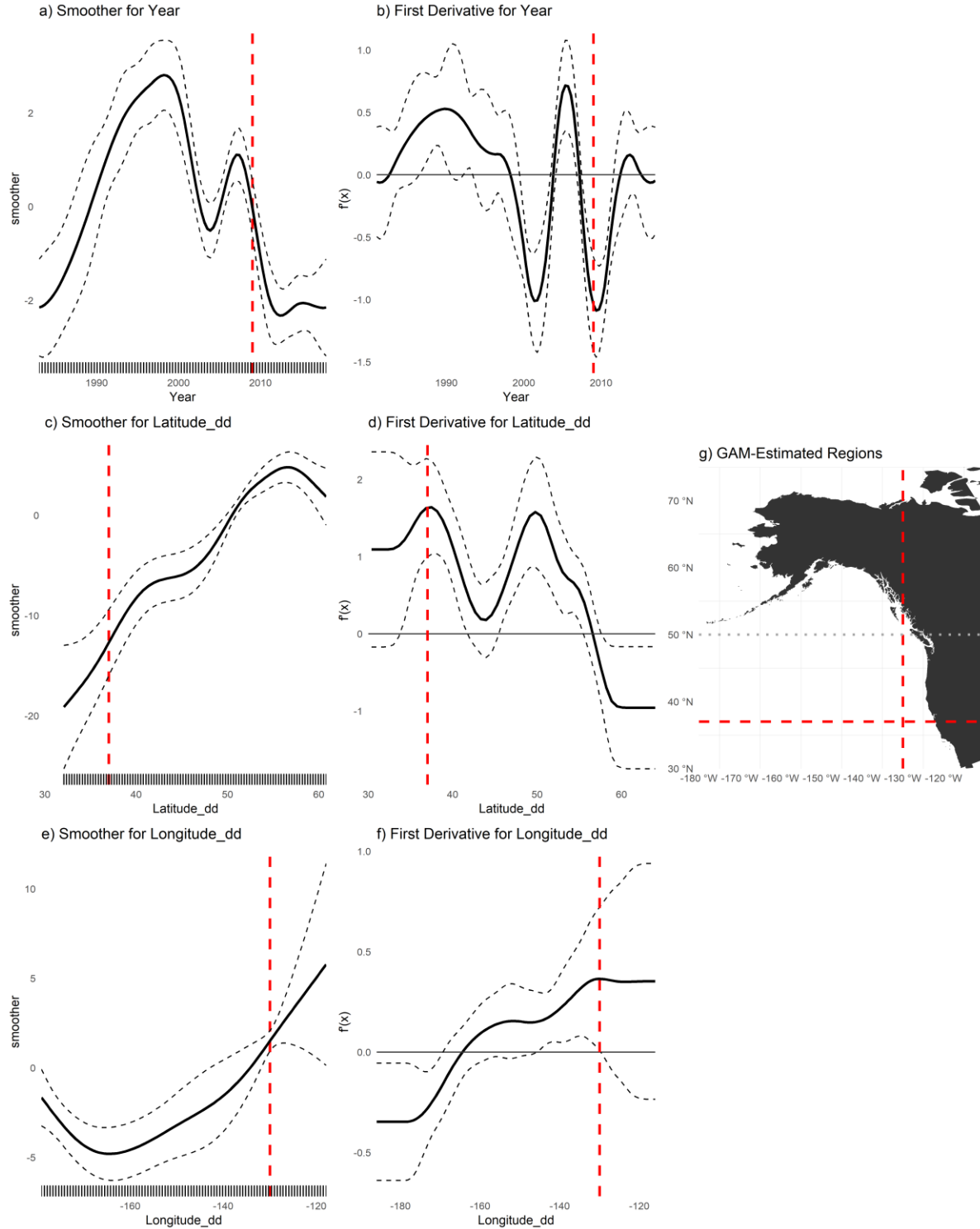


Figure 6. (a,c,e) Plots of smoothers (fitted regression splines) for Year, Latitude, and Longitude, and first derivatives thereof for female age six sablefish (b,d,f). On a-f, vertical dashed lines indicate latitudes, longitudes or years that corresponded to the highest first derivative and had a confidence interval that did not include zero. g) map with model-detected breakpoints (red dashed lines) and breakpoints detected for other ages (grey dotted line).

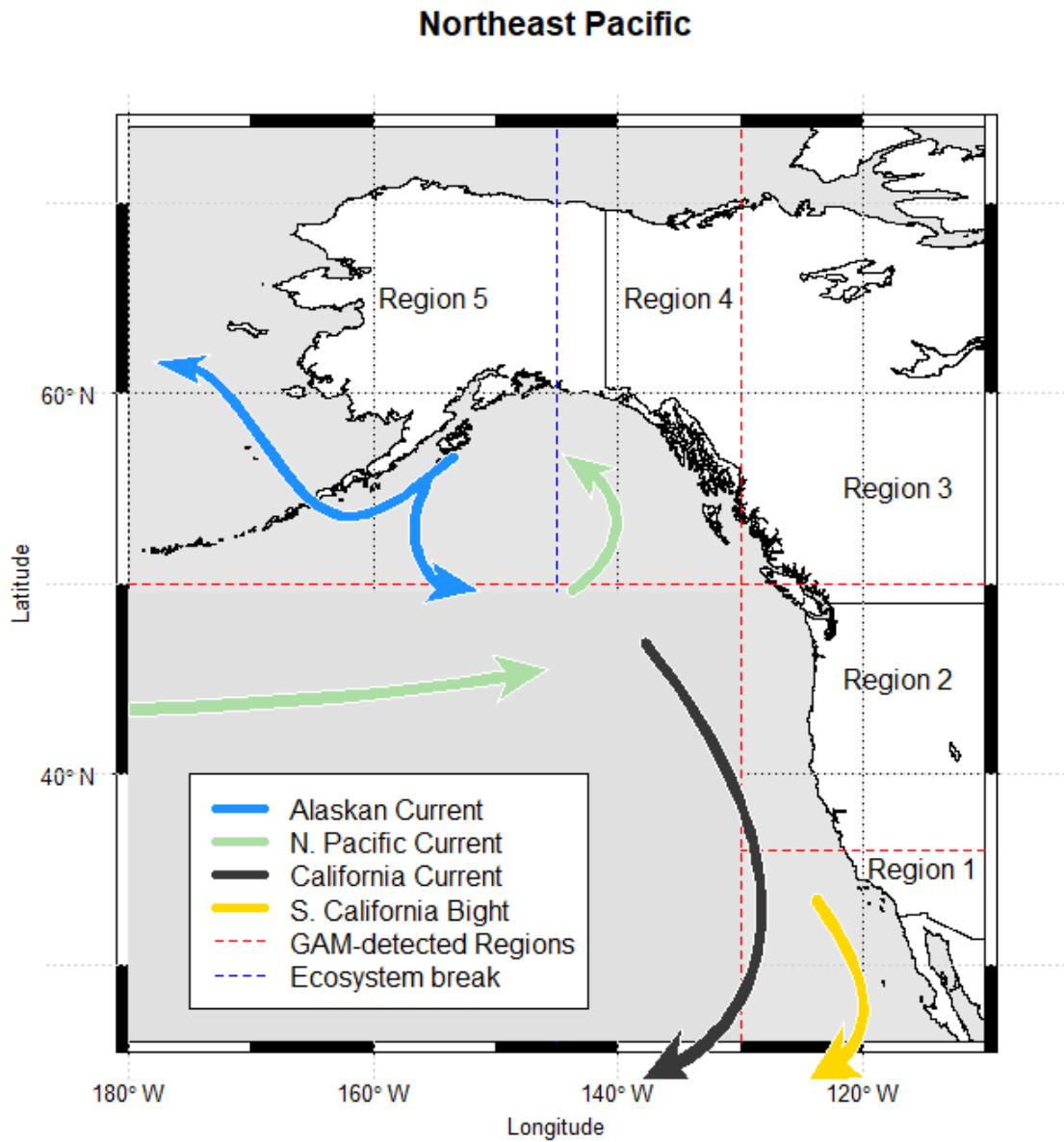


Figure 7. Method-detected breakpoints (red dashed lines) and ecosystem-based break (blue dashed lines) used to delineate growth regions for sablefish. For illustration, points are raw sablefish observations of both sexes at age 30 years. Map made in R using current data from: https://data.amerigeoss.org/en_AU/dataset/major-ocean-currents-arrowpolys-30m-85

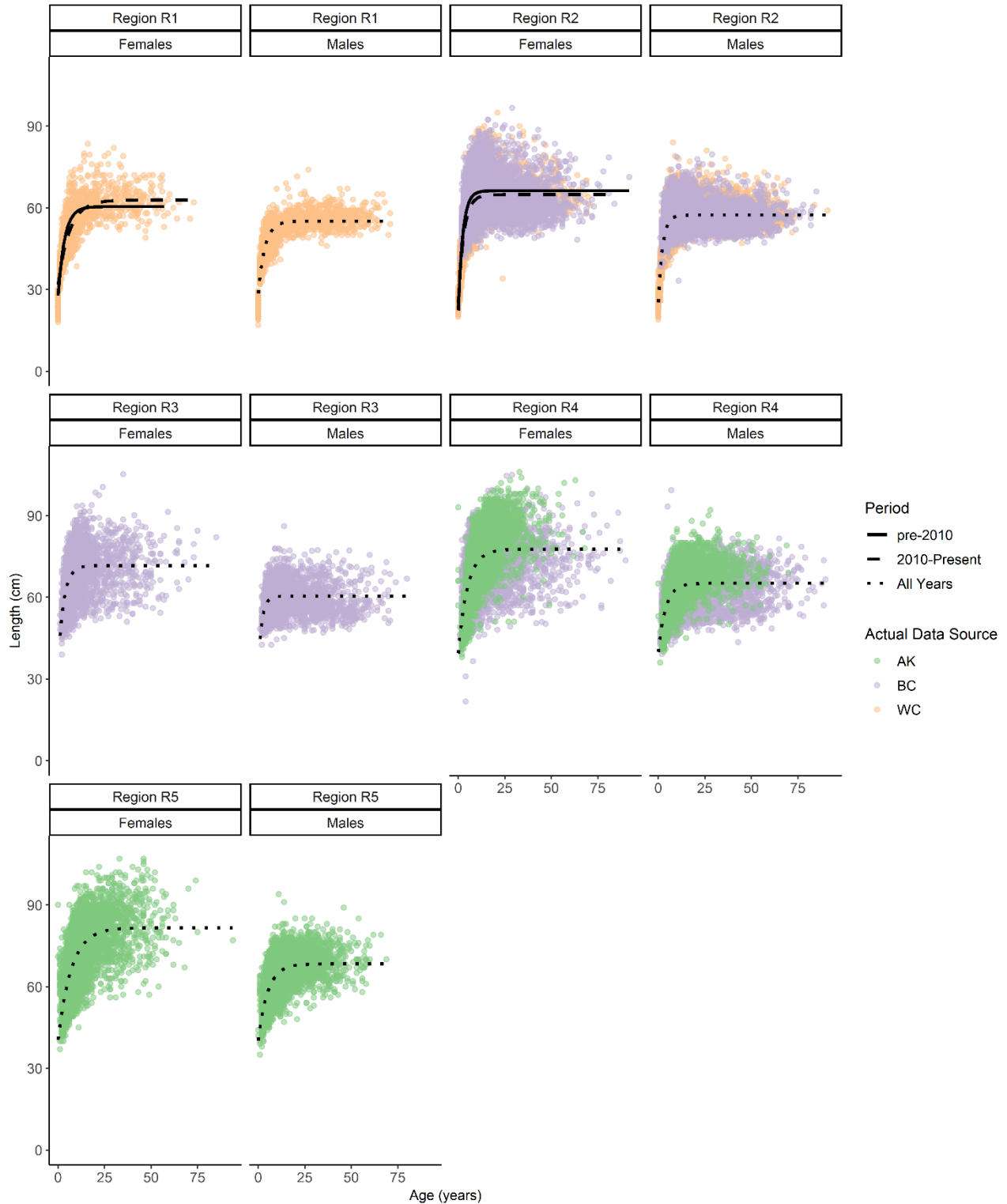


Figure 8. Fits of von Bertalanffy growth function (black lines) to data at the final spatiotemporal aggregation. Points are raw survey data colored by their source. Line types denote whether the fit is for early, late or pooled time period.

Region	Survey Method	Sample size used in this analysis to fit GAM		VBGF parameters from recent stock assessments					
		M	F	L_{∞} (cm)		k (years ⁻¹)		t_0 (years)	
				M	F	M	F	M	F
West Coast of US (Johnson et al., 2015)	Trawl on chartered commercial fishing vessels	7,778	7,222	57	64	0.41	0.32	0 (fixed)	0 (fixed)
British Columbia	Stratified trap survey	6,912	8,088	68.99	72.00	0.29	0.25	32.50	32.50
Alaska Federal (Hanselman et al., 2017)	Longline on chartered commercial fishing vessels	6,818	8,182	*67.8 *65.3	*80.2 *75.6	*0.29 *0.28	*0.22 *0.21	* *2.27	* *1.95

Tables

Table 1. Overview of survey methods, data available and most recent VBGF parameters used for sablefish in stock assessments.

*Time-blocked VBGF parameters for AK Federal assessment 1996-current

*Time-blocked VBGF parameters for AK Federal assessment from 1960-1995 (Hanselman et al., 2017)

Scenario Number	Scenario Description	Stratification
1	No spatial breaks	Latitude and Longitude ~ U[0,50], all fish under regime 1
2	Single, spatial break in middle of range, with no overlap	Latitude and Longitude ~ U[0,25] under regime 1; Latitude and Longitude ~ U[25,50] under regime 2
3	Some overlap between regions	Latitude and Longitude ~ U[0,25] under regime 1; Latitude and Longitude ~ U[20,50] under regime 2
4	Single spatial break at edge of range with no overlap	Latitude ~ U[0,50] for regimes 1 and 2; Longitude ~ U[0,48] for regime 1 Longitude ~ U[48,50] for regime 2
5	Single temporal break at year 50 (of 100); no spatial variability	Latitude and Longitude ~ U[0,50], all fish under regime 1 from years 0 to 49 and regime 2 thereafter

Table 2. Summary of simulation scenarios used to test the proposed method given various degrees of spatial growth variation, and a single temporal scenario.

Region	Sex	Period	Sample size used to fit GAM	Estimated VGBF Parameters			Corresponding estimated endpoints of growth curve	
				L_{∞} (cm)	k (years ⁻¹)	t_0 (years)	L_1 (cm)	L_2 (cm)
1	Female	Early	616	60.44	0.29	-2.15	27.85	60.43
1	Female	Late	699	62.86	0.16	-4.31	31.78	62.63
1	Male	All years	1,314	55.11	0.28	-2.59	28.60	55.11
2	Female	Early	4,913	66.28	0.41	-1.00	22.31	66.28
2	Female	Late	3,356	64.85	0.34	-1.45	25.10	64.85
2	Male	All years	8,871	57.33	0.44	-1.32	25.34	57.33
3	Female	All years	1,640	71.62	0.34	-1.51	35.67	71.62
3	Male	All Years	1,328	60.40	0.51	-1.37	34.23	60.40
4	Female	All years	6,384	77.63	0.20	-3.51	39.46	77.54
4	Male	All years	3,671	65.16	0.26	-3.71	39.90	65.15
5	Female	All years	5,884	81.61	0.14	-4.85	40.47	81.02
5	Male	All years	4,607	68.36	0.20	-4.51	40.18	68.29

Table 3. Description of final spatiotemporal regions, and the sex-specific growth parameters estimated in the analysis. The Region column corresponds to regions depicted in Figure 7, with “early” period being observations before or during 2010, where applicable. Parameter estimates are those used to plot fitted curves in Figure 8.

References

- Adams, G.D., Leaf, R.T., Ballenger, J.C., Arnott, S.A., McDonough, C.J., 2018. Spatial variability in the growth of Sheepshead (*Archosargus probatocephalus*) in the Southeast US: Implications for assessment and management. *Fish. Res.* 206, 35–43. <https://doi.org/10.1016/j.fishres.2018.04.023>
- Austin, M.P., 2002. Spatial prediction of species distribution: An interface between ecological theory and statistical modelling. *Ecol. Modell.* [https://doi.org/10.1016/S0304-3800\(02\)00205-3](https://doi.org/10.1016/S0304-3800(02)00205-3)
- Baumann, H., Conover, D.O., 2011. Adaptation to climate change: Contrasting patterns of thermal-reaction-norm evolution in Pacific versus Atlantic silversides. *Proc. R. Soc. B Biol. Sci.* <https://doi.org/10.1098/rspb.2010.2479>
- Beck, K.K., Fletcher, M.S., Gadd, P.S., Heijnis, H., Saunders, K.M., Simpson, G.L., Zawadzki, A., 2018. Variance and Rate-of-Change as Early Warning Signals for a Critical Transition in an Aquatic Ecosystem State: A Test Case From Tasmania, Australia. *J. Geophys. Res. Biogeosciences.* <https://doi.org/10.1002/2017JG004135>
- Breitburg, D., Craig, J.K., Fulford, R., Rose, K., Boynton, W., Brady, D., Ciotti, B., Diaz, R., Friedland, K., Hagy, J., Hart, D., Hines, A., Houde, E., Kolesar, S., Nixon, S., Rice, J., Secor, D., Targett, T., 2009. Nutrient enrichment and fisheries exploitation: interactive effects on estuarine living resources and their management. *Hydrobiologia* 629, 31–47. <https://doi.org/10.1007/s10750-009-9762-4>
- Conover, D.O., Present, T.M.C., Conover, D., Present, T.M.C., 1990. Countergradient Variation in Growth Rate : Compensation for Length of the Growing Season among Atlantic Silversides from Different Latitudes 83, 316–324.
- Cope, J.M., Punt, A.E., 2007. Erratum: Admitting ageing error when fitting growth curves: an example using the von Bertalanffy growth function with random effects. *Can. J. Fish. Aquat. Sci.* <https://doi.org/10.1139/f07-095>
- Cummins, P.F., Freeland, H.J., 2007. Variability of the North Pacific Current and its bifurcation. *Prog. Oceanogr.* 75, 253–265. <https://doi.org/10.1016/j.pocean.2007.08.006>
- Denson, L.S., Sampson, D.B., Stephens, A., 2017. Data needs and spatial structure considerations in stock assessments with regional differences in recruitment and exploitation. *Can. J. Fish. Aquat. Sci.* 74, 1918–1929. <https://doi.org/10.1139/cjfas-2016-0277>
- Department of Fisheries and Oceans, 2016. A Revised Operating Model for Sablefish (*Anoplopoma fimbria*) in British Columbia, Canada. Dep. Fish. Ocean. Canada, 3190 Hammond Bay Road Nanaimo, BC V9T 6N7. <https://doi.org/http://www.dfo-mpo.gc.ca/csas-sccs/>
- Echave, K.B., Hanselman, D.H., Adkison, M.D., Sigler, M.F., 2012. Interdecadal Change in Growth of Sablefish (*Anoplopoma fimbria*) in the Northeast Pacific Ocean. *Fish. Bull.* 110, 361–374.
- Gertseva, V., Matson, S.E., Cope, J., 2017. Spatial growth variability in marine fish: Example from Northeast Pacific groundfish. *ICES J. Mar. Sci.* 74, 1602–1613. <https://doi.org/10.1093/icesjms/fsx016>
- Goethel, D.R., Berger, A.M., 2017. Accounting for spatial complexities in the calculation of biological reference points: effects of misdiagnosing population structure for stock status indicators. *Can. J. Fish. Aquat. Sci.* 74, 1878–1894. <https://doi.org/10.1139/cjfas-2016-0290>
- Guthery, F.S., Burnham, K.P., Anderson, D.R., 2003. Model Selection and Multimodel

- Inference: A Practical Information-Theoretic Approach. *J. Wildl. Manage.*
<https://doi.org/10.2307/3802723>
- Hanselman, D.H., Heifetz, J., Echave, K.B., Dressel, S.C., Jech, J.M., 2015. Move it or lose it: movement and mortality of sablefish tagged in Alaska. *Can. J. Fish. Aquat. Sci.* 72, 238–251. <https://doi.org/10.1139/cjfas-2014-0251>
- Hanselman, D.H., Lunsford, C.R., Rodgveller, C.J., 2017. Assessment of the sablefish stock in Alaska in 2017. *Natl. Mar. Fish. Serv. Auke Bay Mar. Stn.* 11305 Glacier Highw. Juneau, AK 99801 576–717.
- Hilborn, R., Mente-Vera, C. V., 2008. Fisheries-induced changes in growth rates in marine fisheries: Are they significant?, in: *Bulletin of Marine Science*.
- Houde, E.D., 1989. Comparative growth, mortality, and energetics of marine fish larvae: temperature and implied latitudinal effects. *Fish. Bull.* 87, 471–495.
- Hurst, T.P., Abookire, A.A., 2006. Temporal and spatial variation in potential and realized growth rates of age-0 year northern rock sole. *J. Fish Biol.* 68, 905–919.
<https://doi.org/10.1111/j.0022-1112.2006.00985.x>
- Jasonowicz, A.J., Goetz, F.W., Goetz, G.W., Nichols, K.M., 2017. Love the one you're with: genomic evidence of panmixia in the sablefish (*Anoplopoma fimbria*). *Can. J. Fish. Aquat. Sci.* 74, 377–387. <https://doi.org/10.1139/cjfas-2016-0012>
- Johnson, K.F., Rudd, M.B., Pons, M., Akselrud, C.A., Lee, Q., Haltuch, M.A., Hamel, O.S., 2015. Status of the U.S. sablefish resource in 2015. 3National Marine Fisheries Service Northwest Fisheries Science Center 2725 Montlake Blvd. E. Seattle WA, 98122.
- Jonassen, T.M., Imsland, A.K., Fitzgerald, R., Bonga, S.W., Ham, E. V., Nævdal, G., Stefánsson, M.O., Stefánsson, S.O., 2000. Geographic variation in growth and food conversion efficiency of juvenile Atlantic halibut related to latitude. *J. Fish Biol.* 56, 279–294.
<https://doi.org/10.1006/jfbi.1999.1159>
- Kim, H.J., Miller, A.J., McGowan, J., Carter, M.L., 2009. Coastal phytoplankton blooms in the Southern California Bight. *Prog. Oceanogr.* 82, 137–147.
<https://doi.org/10.1016/j.pocean.2009.05.002>
- King, J.R., McFarlane, G.A., Beamish, R.J., 2001. Incorporating the dynamics of marine systems into the stock assessment and management of sablefish. *Prog. Oceanogr.* 49, 619–639.
[https://doi.org/10.1016/S0079-6611\(01\)00044-1](https://doi.org/10.1016/S0079-6611(01)00044-1)
- Kristensen, K., Nielsen, A., Berg, C., Skaug, H., Bell, B., 2016. TMB: Automatic Differentiation and Laplace Approximation. *ournal Stat. Softw.* 70, 1–21.
<https://doi.org/10.18637/jss.v070.i05>
- Levins, R., 1968. *Evolution in Changing Environments., Population Studies.* Princeton University Press. <https://doi.org/10.2307/2173276>
- Mackas, D.L., Thomson, R.E., Galbraith, M., 2011. Changes in the zooplankton community of the British Columbia continental margin, 1985-1999, and their covariation with oceanographic conditions. *Can. J. Fish. Aquat. Sci.* 58, 685–702.
<https://doi.org/10.1139/f01-009>
- Mason, J.C., Beamish, R.J., McFarlane, G.A., 1983. Sexual Maturity, Fecundity, Spawning, and Early Life History of Sablefish (*Anoplopoma fimbria*) off the Pacific Coast of Canada. *Can. J. Fish. Aquat. Sci.* <https://doi.org/10.1139/f83-247>
- McDevitt, M., 1990. *Growth Analysis of Sablefish From Mark-Recapture Data From the Northeast Pacific.* University of Washington.
- McGarvey, R., Fowler, A.J., 2002. Seasonal growth of King George whiting (*Sillaginodes*

- punctata) estimated from length-at-age samples of the legal-size harvest. *Fish. Bull.* 100, 545–558.
- Northwest Fisheries Science Center, 2019. West Coast Groundfish Bottom Trawl Survey Data - Annual West Coast time series groundfish trawl data collection survey from 2010-06-15 to 2010-08-15. [WWW Document]. URL https://www.nwfsc.noaa.gov/research/divisions/fram/groundfish/bottom_trawl.cfm
- Pacific Fisheries Management Council (PFMC), 2013. Pacific Coast Fishery Ecosystem Plan for the U.S. Portion of the California Current Large Marine Ecosystem. Pacific Fish. Manag. Counc. 7700 NE Ambassad. Place, Suite 101, Portland, Oregon, 97220.
- Perretti, C.T., Thorson, J.T., 2019. Spatio-temporal dynamics of summer flounder (*Paralichthys dentatus*) on the Northeast US shelf. *Fish. Res.* 215, 62–68. <https://doi.org/10.1016/j.fishres.2019.03.006>
- Pörtner, H.O., Knust, R., 2007. Climate change affects marine fishes through the oxygen limitation of thermal tolerance. *Science* (80-.). <https://doi.org/10.1126/science.1135471>
- Punt, A.E., 2019. Spatial stock assessment methods: A viewpoint on current issues and assumptions. *Fish. Res.* <https://doi.org/10.1016/j.fishres.2019.01.014>
- Punt, A.E., 2003. The performance of a size-structured stock assessment method in the face of spatial heterogeneity in growth. *Fish. Res.* 65, 391–409. <https://doi.org/10.1016/j.fishres.2003.09.028>
- R Development Core Team, R., 2011. R: A Language and Environment for Statistical Computing, R Foundation for Statistical Computing. <https://doi.org/10.1007/978-3-540-74686-7>
- Ricker, W., 1969. Effects of size-selective mortality and sampling bias on estimates of growth, mortality, production and yield. *J. Fish. Res. Board Canada.* <https://doi.org/10.1139/f69-051>
- Rodionov, S., Overland, J.E., 2005. Application of a sequential regime shift detection method to the Bering Sea ecosystem. *ICES J. Mar. Sci.* 62, 328–332. <https://doi.org/10.1016/j.icesjms.2005.01.013>
- Rodionov, S.N., 2004. A sequential algorithm for testing climate regime shifts. *Geophys. Res. Lett.* 31, 2–5. <https://doi.org/10.1029/2004GL019448>
- Rutecki, L., Rodgveller, C.J., Lunsford, C.R., 2016. National Marine Fisheries Service Longline Survey Data Report and Survey History , 1990-2014. 17109 Lena Point Loop Road Juneau, AK 99801. <https://doi.org/10.7289/V5/TM-AFSC-324>
- Schnute, J., 1981. A Versatile Growth Model with Statistically Stable Parameters. *Can. J. Fish. Aquat. Sci.* 38, 1128–1140. <https://doi.org/10.1139/f81-153>
- Shotwell, S.K., Hanselman, D.H., Belkin, I.M., 2014. Toward biophysical synergy: Investigating advection along the Polar Front to identify factors influencing Alaska sablefish recruitment. *Deep. Res. Part II* 107, 40–53. <https://doi.org/10.1016/j.dsr2.2012.08.024>
- Siddon, E., Zador, S., 2018. Ecosystem Status Report 2018: Eastern Bering Sea. North Pacific Fish. Manag. Counc. 605 W. 4th Ave. Suite 306 Anchorage, AK 99301.
- Simpson, G.L., 2018. Modelling palaeoecological time series using generalized additive models. *bioRxiv.* <https://doi.org/10.1101/322248>
- Somers, K.A., Pfeiffer, L., Miller, S., Morrison, W., 2018. Using Incentives to Reduce Bycatch and Discarding: Results Under the West Coast Catch Share Program. *Coast. Manag.* 46, 621–637. <https://doi.org/10.1080/08920753.2018.1522492>
- Stawitz, C.C., Essington, T.E., Branch, T.A., Haltuch, M.A., Hollowed, A.B., Spencer, P.D., 2015. A state-space approach for detecting growth variation and application to North

- Pacific groundfish. *Can. J. Fish. Aquat. Sci.* 72, 1316–1328. <https://doi.org/10.1139/cjfas-2014-0558>
- Stawitz, C.C., Haltuch, M.A., Johnson, K.F., Sciences, F., Fisheries, N., Marine, N., Service, F., Oceanographic, N., 2019. How does growth misspecification affect management advice derived from an integrated fisheries stock assessment model? *Fish. Res.* 213, 12–21. <https://doi.org/10.1016/j.fishres.2019.01.004>
- Taylor, B.M., Brandl, S.J., Kapur, M., Robbins, W.D., Johnson, G., Huveneers, C., Renaud, P., Choat, J.H., 2018. Bottom-up processes mediated by social systems drive demographic traits of coral-reef fishes. *Ecology* 99, 642–651. <https://doi.org/10.1002/ecy.2127>
- Thorson, J.T., 2019a. Guidance for decisions using the Vector Autoregressive Spatio-Temporal (VAST) package in stock, ecosystem, habitat and climate assessments. *Fish. Res.* <https://doi.org/10.1016/j.fishres.2018.10.013>
- Thorson, J.T., 2019b. Guidance for decisions using the Vector Autoregressive Spatio-Temporal (VAST) package in stock, ecosystem, habitat and climate assessments. *Fish. Res.* 210, 143–161. <https://doi.org/10.1016/j.fishres.2018.10.013>
- Thorson, J.T., Shelton, A.O., Ward, E.J., Skaug, H.J., 2015. Geostatistical delta-generalized linear mixed models improve precision for estimated abundance indices for West Coast groundfishes. *ICES J. Mar. Sci.* 72, 1297–1310. <https://doi.org/10.1093/icesjms/fsu243>
- Trip, E.L., Choat, J.H., Wilson, D.T., Robertson, D.R., 2008. Inter-oceanic analysis of demographic variation in a widely distributed Indo-Pacific coral reef fish. *Mar. Ecol. Prog. Ser.* 373, 97–109. <https://doi.org/10.3354/meps07755>
- von Bertalanffy, L., 1957. Quantitative Laws in Metabolism and Growth. *Q. Rev. Biol.* <https://doi.org/10.1086/401873>
- Wickham, H., Francois, R., Henry, L., Muller, K., 2019. dplyr: A Grammar of Data Manipulation.
- Williams, A.J., Farley, J.H., Hoyle, S.D., Davies, C.R., Nicol, S.J., 2012. Spatial and sex-specific variation in growth of albacore tuna (*Thunnus alalunga*) across the South Pacific Ocean. *PLoS One* 7. <https://doi.org/10.1371/journal.pone.0039318>
- Wood, S.N., 2011. Fast stable restricted maximum likelihood and marginal likelihood estimation of semiparametric generalized linear models. *J. R. Stat. Soc. Ser. B Stat. Methodol.* <https://doi.org/10.1111/j.1467-9868.2010.00749.x>
- Wood, S.N., 2003. Thin plate regression splines. *J. R. Stat. Soc. Ser. B Stat. Methodol.* <https://doi.org/10.1111/1467-9868.00374>
- Wyeth, M.R., Kronlund, A.R., Elfert, M., 2005. Summary of the 2005 British Columbia Sablefish (*Anoplopoma fimbria*) Research and Assessment Survey Canadian Technical Report of Fisheries and Aquatic Sciences 2694. Science Branch, Pacific Region Pacific Biological Station Nanaimo, British Columbia V9T 6N7.

Acknowledgments

The authors would like to thank Owen Hamel and Christine Stawitz of the Northwest Fisheries Science Center for their thoughtful comments that greatly improved this manuscript. We'd like to thank John Best (SAFS) for suggesting the GAM derivative method as a possible technique, and for the entire Pacific Sablefish Transboundary Assessment Team for their support and feedback on this work. This publication was [partially] funded by the Joint Institute for the Study of the Atmosphere and Ocean (JISAO) under NOAA Cooperative agreement No. NA15OAR4320063, Contribution No. **xxxx-xxx**.

Supplementary material for on-line publication only

[Click here to download Supplementary material for on-line publication only: kapur_etal_S1_appx.docx](#)